ELSEVIER

Physica C 384 (2003) 297–306

PHYSICA C

www.elsevier.com/locate/physc

Collective dynamics of Josephson fluxons in $Bi_2Sr_2CaCu_2O_{8+\delta}$ intrinsic junctions

Dong-In Chang [a], Myung-Ho Bae [a], Hyun-Sik Chang [a], Hu-Jong Lee [a,*], Jinhee Kim [b], Byung-Chill Woo [b], M. Oda [c]

[a] *Department of Physics, Pohang University of Science and Technology, Pohang 790-784, South Korea*
[b] *Electricity Group, Korea Research Institute of Standards and Science, Taejon 305-600, South Korea*
[c] *Department of Physics, Hokkaido University, Sappore 060-0810, Japan*

Received 8 February 2002; received in revised form 28 May 2002; accepted 19 July 2002

Abstract

The dynamic characteristics of Josephson fluxons in naturally stacked intrinsic Josephson junctions in $Bi_2Sr_2CaCu_2O_{8+\delta}$ single crystals were studied experimentally. The Josephson fluxons were generated either by irradiating microwaves or by applying dc magnetic fields in parallel with the junction planes. In the presence of a finite tunneling bias current the fluxons are driven along the junctions in resonance with the excitation modes of Josephson plasma and thus exhibit a variety of dynamic characteristics. Thus in the flux-flow state of fluxons in both cases above, for a relatively low vortex density, sub-branch splitting of the 'supercurrent' branch in the current–voltage (I–V) characteristics was observed, which corresponded to different plasma excitation modes. For a higher vortex density, on the other hand, all the quasiparticle branches merged into a single non-hysteretic I–V curve which exhibited step-like kink features, very similar to the recently predicted ones corresponding to different moving fluxon patterns. The detailed agreement with the theoretical prediction, however, is yet to be confirmed.

PACS: 74.50.+r; 74.72.Hs; 74.80.Dm; 85.25.Cp
Keywords: Fluxon dynamics; Intrinsic Josephson junctions; Plasma excitation modes; Superradiant state

1. Introduction

Collective fluxon dynamics in stacked long Josephson junctions, either artificial or intrinsic, has recently been studied extensively [1–20], mainly because of the high possibility of being applied to high-frequency devices such as THz local oscillators and mixers. Stacked long Josephson junctions also provide ideal systems to study the non-linear dynamic phenomena. Appreciable interlayer coupling leading to the collective behavior can be achieved in such systems by the inductive interaction between adjacent junctions [3–7], if the superconducting layers are thinner than the London penetration depth. Capacitive [8] and non-equilibrium [9] effects may also contribute to the interlayer coupling for thin superconducting layers.

* Corresponding author. Tel.: +82-54-279-2072; fax: +82-54-279-5564.
E-mail address: hjlee@postech.ac.kr (H.-J. Lee).

0921-4534/02/$ - see front matter
PII: S0921-4534(02)01886-5

The fluxon lines generated along the insulating layers by an external magnetic field applied in parallel with the junction planes are driven in a tunneling bias current along the junctions and excite the Josephson plasma oscillations propagating inside the junctions. In contrast to a single junction where only a transverse plasma mode is excited, stacked Josephson junctions exhibit a mixture of both longitudinal and transverse Josephson plasma modes and thus their fluxon dynamics becomes far richer with different dispersions [7,12,13]. The plasma oscillations are converted into the electromagnetic radiation at a boundary of stacked junctions. Thus, a mesa of long Josephson junctions in a flux-flow mode can be utilized as a THz-range local oscillator [14].

Highly anisotropic high-T_c superconducting materials such as $Bi_2Sr_2CaCu_2O_{8+x}$ (Bi2212) provide natural atomic-scale stacks of Josephson junctions [15]. The interlayer coupling in these intrinsic Josephson junctions (IJJs), because of the extreme thinness of the junction unit, can be a few orders of magnitude stronger than in artificially stacked junctions. Studies on stacks of IJJs revealed a variety of interesting phenomena such as geometric resonance [21], non-Josephson radiation [22], and sub-branch splitting [16,17]. In general, in a certain condition, stable in-phase locking of vertically stacked Josephson junctions can be established [3,4,7,8,10,11,23,24]. The radiation from this phase-locked state of stacked IJJs can be phase-coherent and far more intensive than from a single-junction Josephson oscillator. Thus, clear understanding of the interplay between the fluxon motion and the characteristic plasma modes is essential for proper device applications of IJJs.

In our previous study multiple sub-branches were observed in the I–V characteristics of stacks of IJJs, when irradiated with a high-power microwave of frequencies higher than the junction plasma frequency [17]. In this case the magnetic-field component of the microwave was believed to generate Josephson fluxons inside the junctions in a long-junction limit. The study indicated that each sub-branch represented a collective motion of microwave-induced Josephson fluxons which was coherent with a plasma excitation mode. Similar branch splitting was obtained by others in a mesa of Bi2212 IJJs with dc magnetic fields applied in parallel with the *ab* plane [16] and also attributed to a specific mode of coherent Josephson fluxon motion. In their study, however, the number of identified sub-branches ($\lesssim 10$) was far smaller than the number of IJJs in the mesa ($\gtrsim 200$). Strong pinning of fluxons by quenched disorder in the junctions may have prevented development of a fully collective motion of fluxons over the whole mesa. The observed discrepancy suggests that it is important to investigate the interrelation between the behavior of the microwave-generated fluxons and that of the dc-field-generated ones. In this study we thus used *an identical mesa* to measure and compare the fluxon behaviors of both cases. As in our previous observation, in this mesa (UD1), we obtained sub-branch splitting for high-power microwaves corresponding to effective magnetic fields of a few tens mT. We also observed similar sub-branch splitting in relatively low dc magnetic fields below 1 T. In spite of some differences in the detailed features to be discussed below observed results suggest that the sub-branch splitting of the two cases is a consequence of collective fluxon motion which is resonant with the different plasma excitation modes.

Simulation studies by others also indicate that the spatial flux-flow structure inside a stack of Josephson junctions is sensitive to the vortex density and the driving tunneling current [12,18, 19]. In a given magnetic field the fluxon pattern is predicted to be more ordered and stable in a higher driving current until the fluxon velocity matches the fastest transverse mode velocity of plasma excitation. For a certain range of current in relatively high magnetic fields driven fluxons form a rectangular lattice. This moving fluxon pattern can excite the locked in-phase plasma oscillations over all junctions, which will lead to the so-called 'super-radiant' state with strong and sharp emission power [12,18,19]. Thus IJJs may provide natural realization of highly efficient high-frequency oscillators. In this study we thus also investigated the characteristics revealed in the I–V curves in high magnetic fields of the same mesa (UD1) of IJJs used for the study of fluxon modes and of mesas (AG1 and AG2) prepared on an as-grown single crystal. We observed step-like kinks in the I–V

curves which were reminiscent of the features caused by the different moving fluxon patterns in a finite tunneling bias current [12,18,19] but the detailed agreement with the theoretical prediction is still inconclusive.

2. Experimental

In this study, we prepared mesas on the planar surface of Bi2212 single crystals, both underdoped (mesa UD1) and as-grown (mesas AG1 and AG2). A microwave can be applied uniformly to a stack of IJJs for its frequency higher than the Josephson plasma frequency. Since the available microwave frequency in our experiment was in the range of 70–95 GHz while the plasma frequency of as-grown Bi2212 single crystals was in the range of 150–200 GHz we reduced the Josephson plasma frequency of stacked junctions by reducing the doping level of the crystals and thus weakening the interlayer coupling. As-grown and underdoped single crystals were prepared by the standard solid-state-reaction method and by the process described in Ref. [25], respectively. We used both underdoped mesa (UD1) and as-grown mesas (AG1, AG2) to study the dynamics of field-generated fluxons. The following is a brief description of the mesa fabrication process, the details of which are described elsewhere [20,25]. A Au film, a-few-thousand-Å in its thickness, was first deposited on the surface of a freshly cleaved single crystal. Mesa structure was then photolithographically patterned and ion-beam etched. Contact leads were attached to the mesa by additional photolithographic patterning, metal deposition, and ion-beam etching. Finally, the central mesa (refer to the inset of Fig. 1) of typical lateral dimension of 10×45 μm^2 was divided into equal halves by further etching it with the contact leads as masks. The dimension of each smaller mesa thus prepared in the central mesa was 10×13 μm^2. The total thickness of the central mesa was usually less than 200 Å.

All the measurements were done in a standard four-terminal configuration shown schematically in the inset of Fig. 1, with a low-pass filter connected to each electrode terminal located at room temperature. We took sequentially the zero-field

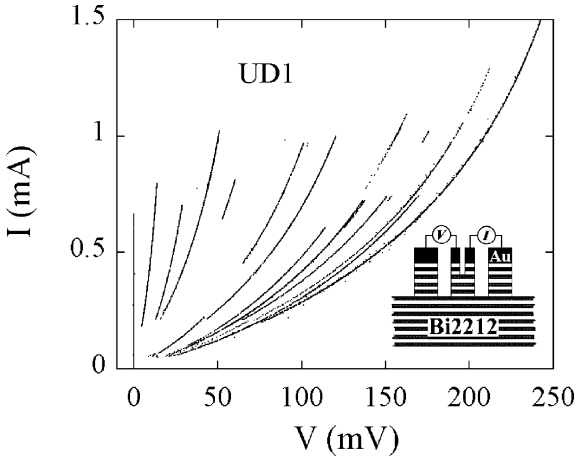

Fig. 1. Zero-field I–V curves taken at $T = 4.2$ K of the mesa UD1 which contains 12 intrinsic junctions. Inset: a four-terminal measurement configuration for the central mesa of the lateral dimensions of 10×45 μm^2.

tunneling resistive transition and the I–V characteristics, and the I–V characteristics in various external magnetic fields applied in parallel with the plane direction, all in an identical setup. In this setup the sample was placed inside a vacuum can which was immersed into liquid helium bath. Magnetic fields parallel to the conducting layers were supplied by a superconducting solenoid, operating in a persistent-current mode. Since applying a field in absolute parallel with the conducting planes is utterly important in this study special care was taken to align a field to conducting planes, following the method in Ref. [26]. Near the angle of parallel alignment a mesa does not exhibit c-axis resistance because the Josephson vortices are pinned to the pancake vortices produced by the vertical component of slightly tilted external field. As the misalignment is reduced in such a way that the c-axis component of the external field becomes lower than the threshold value of c-axis magnetic field entry, however, a sudden appearance of the c-axis resistance takes place due to depinning of the Josephson vortices. Thus, for higher external field, the maximum value of the resultant c-axis resistance increases with the sharpened alignment range of angle. In this study the final alignment was done in a field of 0.5 T at 59 K with the alignment resolution of 0.01 degree.

For the investigation of fluxon dynamics under microwave irradiation, the sample UD1 was warmed up to room temperature. The sample was then put into a different setup and recooled, where it was directly immersed into liquid helium bath. No noticeable change of sample characteristics was observed during this recycling process. A microwave generated by a Gunn diode was transmitted through a rectangular waveguide and coupled inductively to the mesa placed at $\lambda/4$ distance from the end of the waveguide. The maximum nominal microwave output power of the Gunn diode was about 100 mW for the operating frequency of $f = 76$ GHz and the power coupled to the mesa was tuned by using a level-set attenuator.

3. Results and discussion

The c-axis transport of the mesa UD1 showed a clear tunneling conduction behavior, with the resistance increasing sharply with decreasing temperature, typical characteristics of underdoped cuprate single crystals. The onset temperature of the superconducting transition of the mesa was about 83.0 K and the transition width by the 10–90%-transition criterion was 1.3 K. The I–V data of the mesa taken at 4.2 K (Fig. 1) show a superconducting branch and the usual multiple quasiparticle branches. More irregularities with uneven critical currents among different junctions are seen in the I–V data than from as-grown single crystals, supposedly due to the defects introduced during the process of reducing the doping level. The average characteristic voltage jump V_c between the adjacent quasiparticle branches upon exceeding I_c's of junctions is about 17.5 meV. The mesa is seen to contain 12 intrinsic junctions, which is in agreement with the number of junctions estimated from the etching time. The junction giving rise to the supercurrent branch is the one with the weakest Josephson coupling, whose critical current is 0.67 mA. It corresponds to the junction critical current density of 150 A/cm^2 and the Josephson plasma frequency of 39 GHz [27] which is sufficiently lower than the driving frequency of 76 GHz. The reduced hole doping of the Cu–O bilayers [28] contributes to the overall suppression of the superconductivity in the conducting layers and weakening of the resultant interlayer coupling.

As observed in our previous measurements [17] the mesa supports a finite critical current I_c even with microwave irradiation (Fig. 2(a)). With increasing the microwave power the supercurrent branch with a finite critical current changes into a resistive state. Thus, it indicates that the micro-

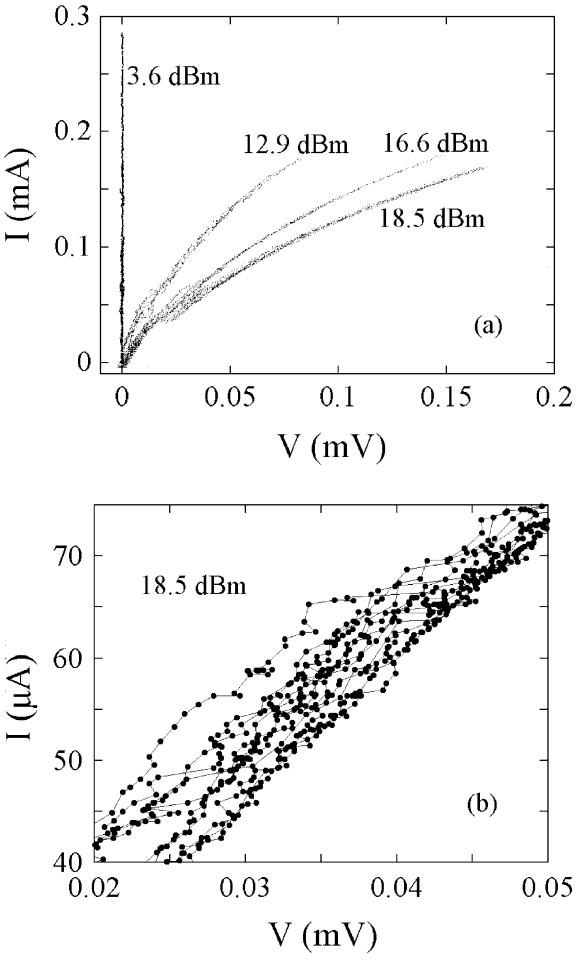

Fig. 2. (a) The evolution of the 'supercurrent' branch of the mesa UD1 at $T = 4.2$ K with increasing the irradiation power of a 76 GHz microwave. (b) An enlarged view of the multiple sub-branches for $P = 18.5$ dBm. The lines are guides to the eyes.

wave-induced fluxons in the mesa were collectively depinned at a certain onset irradiation power. In this mesa the zeroth branch ('supercurrent branch') from the most weakly coupled Josephson junction is resistive for microwave power above 12.9 dBm. At the same time one can notice the appearance of the sub-branch splitting. Fig. 2(b) shows the details of the I–V curve for 18.5 dBm irradiation power, in the voltage range between 0.02 and 0.05 mV. The curve was taken by sweeping the bias current back and forth repeatedly until all the sub-branches were revealed. For this process we used a home-made battery-powered constant-current source with the output resolution of 50 nA or better. Although each sub-branch is not so clearly differentiable as in previous measurements with HgI_2-intercalated Bi2212 single crystals [17], supposedly due to increased defects in the underdoped crystal, the number of sub-branches appears not to deviate much from the total number of IJJs in the mesa, 12. The general feature of the curve is consistent with the previous observations in mesas of HgI_2-intercalated single crystals, where it was concluded that each sub-branch represented a collective motion of microwave-induced Josephson fluxons in resonance with the plasma oscillation mode. Note that the I–V curves in Fig. 2(a) and (b) were obtained from a junction with the weakest Josephson coupling. The fact that the I–V curve of a junction was affected by the presence of other junctions in the mesa and split into sub-branches indicates significant interlayer coupling among the IJJs.

We now turn to the features of I–V curves obtained for low dc external magnetic fields applied in parallel with the junction planes. Because of the geometrical peculiarity of the sample mounting block the field was applied in 60° to the longer side of the mesa (refer to the left inset of Fig. 3(a)) so that the effective width of the mesa under study was about 40 μm. Fig. 3(a) illustrates the gradual evolution of the supercurrent branch for increasing field from 0.1 T up to 0.77 T. One notices, first, the critical current of the supercurrent branch persisted even for the highest field used in Fig. 3(a). The critical current was found to disappear only around $H_c = 1$ T (data are not shown), which indicates that at least weak pinning of the Josephson fluxons existed in the mesa.

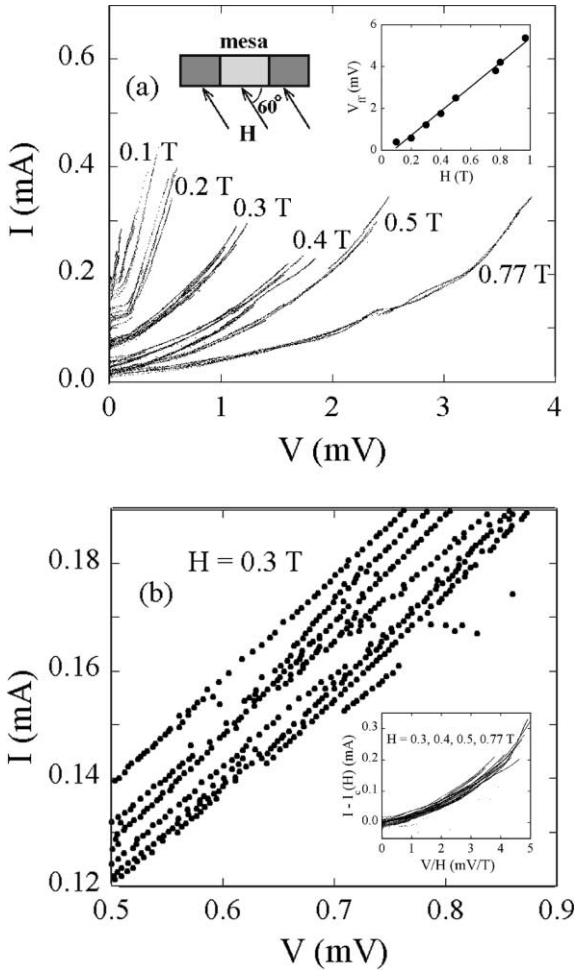

Fig. 3. The evolution of the supercurrent branch of the mesa UD1 in low dc magnetic fields between 0.1 and 0.77 T. The left inset shows the application direction of the transverse magnetic fields relative to the mesa configuration. The right inset shows a linear magnetic-field dependence of the flux-flow voltage V_{ff}, which is defined as the maximum voltage attained by the supercurrent branch for a given magnetic field. (b) The expanded view of the I–V curve at $H = 0.3$ T, showing clear multiple sub-branches. Inset shows the scaling behavior of the flux-flow motion.

Once the fluxons are depinned in a higher bias current an appreciable flux-flow resistance is seen to appear for a field above 0.1 T. One also notices

in Fig. 3(a) that depinned fluxons exhibit the sub-branch splitting. In an external magnetic field similar sub-branch splitting was observed previously in mesas of Bi2212 single crystals [16]. The coherent motion of Josephson vortices in a layered superconductor is expected to result in the sub-branch splitting corresponding to the number of Josephson junctions in the mesa. Fig. 3(b) is an expanded view of the I–V curve at $H = 0.3$ T. Clearly shown is the development of the multiple sub-branches in the supercurrent branch. The identifiable number of sub-branches in the figure is about 8, somewhat smaller than the number of quasiparticle branches, $N = 12$. The I–V curves in an external magnetic field have upturn curvature, which is in agreement with the previous observation [16] but is in contrast to the downturn curvature observed in a mesa under microwave irradiation [17]. This indicates that the behavior of the sinusoidally pulsating fluxons produced by the ac magnetic-field component of a microwave cannot be simulated simply by fluxon motions of an effective dc magnetic field. We believe the irregular interbranch voltage spacing clearly manifested in Fig. 3(b) is due to inhomogeneous distribution of quenched pinning centers along the stacking direction.

Tunneling bias current applied to the IJJs in the mesa causes the Josephson fluxons to move along the junctions, resulting in the flux-flow resistance. Low-intensity external magnetic fields mainly cause the suppression of supercurrent. For the mesa in this study the supercurrent vanishes completely above the critical field $H_c \simeq 1$ T and a resistance in the I–V characteristics starts appearing. Even for a magnetic field smaller than H_c, however, the supercurrent branch becomes resistive at high bias currents. For a magnetic field in the intermediate range of $H_{c1} < H < H_c$ (H_{c1} is the lower critical field of an order several mT), the supercurrent part and the resistive part coexist in the same branch. This feature agrees with the observations by Lee et al. [16] but is in distinction from the result of the microwave irradiation [17], in which the coexistence of the two different characteristic parts was not observed. Instead, microwave-generated fluxons in the power-level corresponding to the effective magnetic field of only a few tens mT exhibit resistive flux-flow behavior as in the low-bias region of each curve in Fig. 2(a), and also in Fig. 2(b) of Ref. [17]. Thus the Josephson fluxons generated by a static magnetic field tend to be more strongly pinned than the microwave-generated fluxons. If we define the flux-flow voltage, V_{ff}, as the maximum voltage attained by the supercurrent branch for a given magnetic field intensity, V_{ff} is almost linearly proportional to H as shown in the right inset of Fig. 3(a), except for the small field offset due to a finite pinning of fluxon lines. This result is consistent with the fact that, in the flux-flow state without pinning, the time-averaged voltage across a junction is proportional to the driven velocity and the number of fluxons in the junction. Thus, if we replot the resistive part of the data in Fig. 3(a) as a function of the reduced voltage V/H the I–V curves for different magnetic fields satisfy a scaling flux-flow behavior as shown in the inset of Fig. 3(b). In the inset the critical current part was subtracted from the total current to compare the resistive part only. This result indicates that the resistive branches in relatively low magnetic fields in Fig. 3(a) indeed resulted from the flux-flow resistance of the field-induced fluxons.

As we further increase the magnetic-field intensity up to the value where the critical current starts disappearing, i.e., about 1 T, the branch-splitting in each quasiparticle branch also starts vanishing, merging into a single quasiparticle curve. For further higher magnetic fields the hysteresis in different quasiparticle branches gradually disappears and all the branches arising from different intrinsic junctions finally merge into a single curve for fields beyond 3–4 T (Fig. 3(a)). In this field range we observed two characteristic step-like 'kinks' in the I–V curves. For a given fluxon density the *first* low-voltage kink as denoted by a thin arrow in Fig. 4(a) is more pronounced than the *second* high-voltage one denoted by a void-head arrow. As seen in the inset of Fig. 4(b) the voltage value of the first kink increases rapidly with increasing the applied magnetic field. By contrast, the voltage value of the second kink increases with magnetic fields in a much lower rate, although a linearity relation looks to exist between

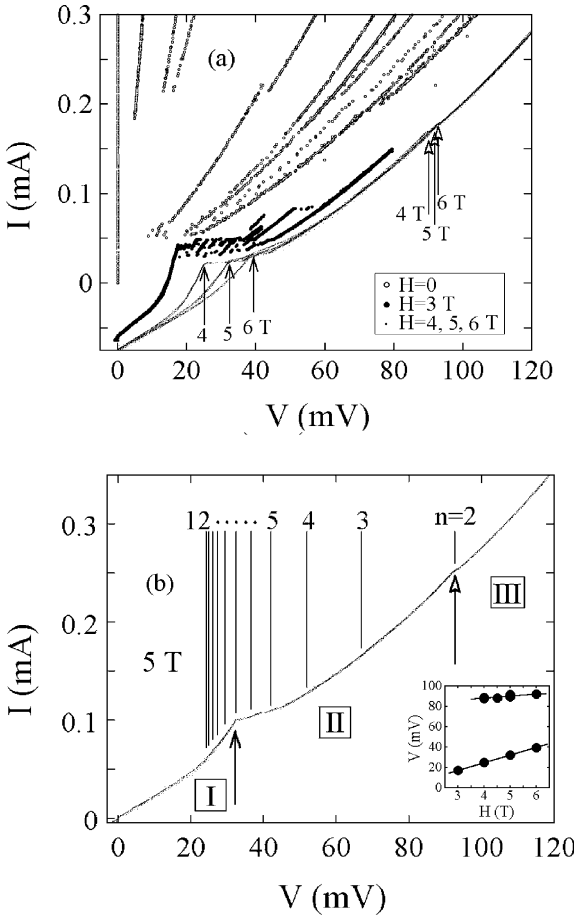

Fig. 4. (a) I–V characteristics of the mesa UD1 in dc magnetic fields of $H = 0$, 3, 4, 5, and 6 T. The curve for 3 T (the ones for 4, 5, and 6 T) is shifted downward by 0.065 mA (by 0.075 mA) for the clarity of illustration. For fields higher than 4 T, quasiparticle branches merge into a single curve which exhibits two characteristic step-like kinks denoted by upward arrows for each field value. (b) Detailed shape of the I–V curve in 5 T, showing more clearly the existence of the two kinks as denoted by the arrows. Each voltage region is explained in the text. The vertical bars denote the flux-flow voltages of the field-induced fluxons which move in resonance with the plasma excitation modes. Inset: the change of the kink positions in (a) with magnetic fields.

the voltage position of a kink and an applied magnetic field.

Numerical studies with coupled sine-Gordon equations [12,18,19] have shown that structural transitions of the moving Josephson-fluxon patterns can take place with a gradual variation of the applied dc magnetic field or the tunneling bias current. Based on the snapshot pattern of the Josephson fluxon array and the power spectrum analysis, the I–V characteristics in a relatively high fluxon density are classified into four regions. The lowest bias region, Region I, is characterized by ω^{-2} dependence of the power spectrum, corresponding to the random distribution and the irregular motion of Josephson fluxons. With an increase of the bias current, Region II is reached where a wavy chain-like moving fluxon distribution is stabilized. The occurrence of the wavy chain-like fluxon pattern indicates that a correlation between fluxons develops. If the bias current increases further, reaching Region III, a rectangular Josephson fluxon lattice appears. In Region III, all the Josephson fluxons in a mesa move in phase, potentially generating a strong radiation of electromagnetic wave. Such a state is called as the 'superradiant' state. Further increase of the bias current makes the rectangular fluxon lattice unstable and in this Region IV the fluxon pattern becomes a modulated triangular lattice. The boundary of any two adjacent regions is revealed as a step-like kink in the I–V curve, similar to the one in Fig. 4(a).

For a clearer illustration of the occurrence of the kinks, we replot in Fig. 4(b) the I–V curve for a field of 5 T. The two upward arrows indicate the positions of the first and the second kinks. The simulation results revealed that the kinks would take place when the fluxons move in resonance with the Josephson plasma modes. In Fig. 4(b) the two resonant points, the boundaries between Regions I and II, and between Regions II and III, appear to be identified. We failed, however, to observe the third kink for the bias current all the way up to 1.5 mA or the corresponding voltage up to about 300 mV. Numerical simulation [18,19] shows that the boundary between Regions III and IV is more difficult to identify than the one between Regions II and III. Highly non-linear behavior of the measured I–V curves, different from that of the resistively shunted junction (RSJ) model used for numerical simulations, makes it even more difficult to identify the boundary between Regions III and IV.

Each resonant point is predicted to satisfy the following dispersion relation [12,18,19].

$$\omega^n(k_x) = \omega_p \sqrt{1 + \frac{\lambda_c^2 k_x^2}{1 + \frac{2\lambda_{ab}^2}{sD}\left(1 - \cos\left(\frac{\pi n}{N+1}\right)\right)}} \qquad (1)$$

Here ω_p is the junction plasma frequency, λ_c and λ_{ab} are the London penetration depths in the *ab* plane and along the *c*-axis, respectively. k_x is the wave number along the width of the junction which should vary in proportion with the applied magnetic field H, and s and D are the thickness of the superconducting and insulating layers, respectively. The mode index n runs from 1 to N, the total number of junctions in a mesa. The unobserved third kink corresponds to the resonant point with $n = 1$ mode, the second kink to $n = 2$ mode, and the lowest-voltage first kink is predicted to almost coincide with the resonant point with $n = N$ mode.

In Fig. 4(b) we plot, by the vertical bars, the expected voltage positions of fluxons which are resonant with the plasma modes for a mesa of 12 IJJs. The number on the top end of each bar denotes the corresponding mode index. Each position was determined using Eq. (1) with the parameter values [3,18] of $\lambda_c = 125$ μm, $\lambda_{ab} = 170$ nm, $s = 0.3$ nm, and $D = 1.2$ nm. Since the third kink corresponding to $n = 1$ is missing in our data the value of ω for the second mode is calculated and positioned in coincidence with the position of the second kink, using the fact that $\omega \propto V$. The positions of the rest of the modes are determined using the calculated ω values in comparison with that for $n = 2$. In this scale the third kink is supposed to take place at 140 mV. The position of the first kink turns out quite close to the expectation. In our data, as can be surmised in Fig. 4(a) and (b), the positions of the kinks tend to be in better agreement with expectation for smaller field values.

We obtained similar high-field *I–V* behavior in the mesa AG2. Zero-field *I–V* characteristics of AG2 in the inset of Fig. 5 are more regular than those of UD1 shown in Fig. 1, suggesting that this mesa fabricated on an as-grown single crystal was more defect-free. The zero-field *I–V* characteristics also indicate that the mesa AG2 contained 12 intrinsic junctions. Illustrated in the main panel of Fig. 5 are high-field *I–V* data for the mesa AG2,

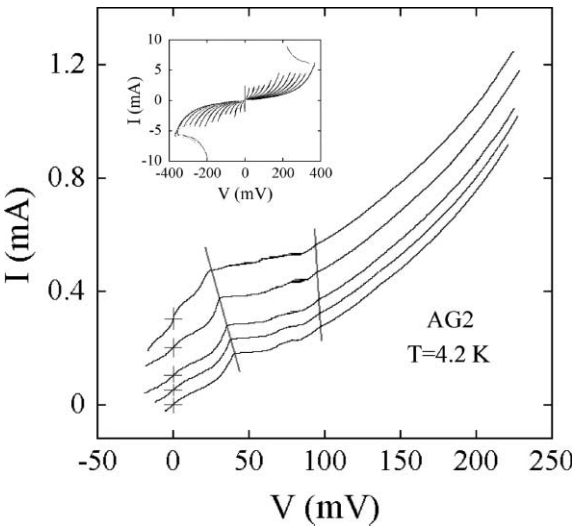

Fig. 5. *I–V* characteristics of the mesa AG2 in dc magnetic fields of $H = 4.0$, 4.5, 5.0, 5.25, and 5.5 T from top to bottom. The curves for 5.0 and 5.25 T (4.0 and 4.5 T) are shifted upward by 0.05 mA (0.1 mA) from the adjacent curves for the clarity of illustration. Inset: *I–V* characteristics of AG2 in zero external field.

corresponding to Fig. 4(a), in magnetic fields from 4 to 5.5 T. The curves are shifted vertically for the sake of clarity. All the curves show kink structure as observed in UD1. The first and the second kinks in each curve (the positions of which are denoted by the two lines) are evident. In this mesa, either, the third kink was not observed. The relative positions of the two kinks in this mesa are almost the same as those in the mesa UD1. Each curve shows some structure in the bias range between the first and the second kinks. This was due to hysteretic quasiparticle branches still persisting in this field range. The hysteretic behavior became more conspicuous in the *I–V* characteristics taken by repeated sweeping of the bias. The two kinks in each curve in the main panel of Fig. 5 were very reproducible in their shapes and in the occurrence positions, which confirmed that those kinks were not caused by the remnant hysteretic quasiparticle branches.

The striking resemblance between the *I–V* curves and the simulation results looks to suggest the existence of the structural transition of the moving fluxon pattern with an increase of the bias

current. Then the Region III denoted in Fig. 4(b) would correspond to the predicted superradiant state. Closer examination of Fig. 4(a) and Eq. (1), however, reveals a serious discrepancy between the observed results for the mesa UD1 and the expectation. Since the second term in the square root of Eq. (1) is much larger than 1 for IJJs the value of ω changes almost in proportion to H, which is in agreement with the trend of the voltage positions of the two kinks in Fig. 4(a) or in the inset of Fig. 4(b). But, at the same time, Eq. (1) predicts that the increase of ω with H should be larger in a resonant mode with a lower index number, which is in clear contradiction to the results in Fig. 4(a) or in the inset of Fig. 4(b). The quenched disorder in the junctions may have affected the results. But the trend did not change in the mesa AG2, either, which presumably contained less defect than UD1. Thus, we cannot rule out the possibility that the features in Fig. 4(a) and (b) may not correspond to the assumed moving fluxon patterns. Although the picture of the transformation of the fluxon configuration with the bias current in the two mesas studied looks quite plausible the issue is not fully settled yet. Further study is necessary to clarify more precise nature of the kinks and any connection to the moving vortex structures.

To draw more definitive conclusion on the fluxon dynamics one needs to study on mesas with boundary conditions closer to those of theoretical consideration. It is necessary to make the width of a mesa comparable to the Josephson penetration depth so that the mesa is to put in a one-dimensional limit as in the cases of any theoretical consideration carried out to date. One also needs to remove the large pedestal part of a single crystal below a mesa under study to minimize any interference of the fluxons in the pedestal part with the dynamics of fluxons in the mesa. This may be achieved by adopting the double-side-cleaving technique developed recently [29].

The observation of the third kink is utterly important because it will give a more concrete evidence that the observed kinks are related with the vortex state. In a practical point of view we are particularly interested in the so-called 'superradiant' vortex state [12,18,19] in Region III, because it is closely related to devising THz-range radiation sources. The radiation may be directly detected by placing a detector mesa close to a radiator mesa and observing the resulting Shapiro steps.

4. Conclusion

In summary, we observed multiple sub-branches in the I–V characteristics of stacks of IJJs, with the application of both microwaves and magnetic fields. The ac magnetic field component of the microwave induces the pulsating Josephson fluxons. With microwave irradiation sub-branch splitting was most clearly revealed for effective magnetic fields in the range of a few tens mT. But in an external dc magnetic field the branch splitting was exhibited most clearly for several tenth of tesla and disappeared for fields beyond 1 T. In a further higher field region, all the quasiparticle branches merged into a single branch and the I–V characteristics became non-hysteretic. The I–V characteristics at the high-field region exhibited two step-like kinks which possessed striking resemblance to the expected simulation results corresponding to the structural transitions of moving fluxon patterns. Detailed analysis of the data for the mesas fabricated both on underdoped as well as as-grown single crystals, however, showed a discrepancy between the observation and the simulation. A more direct means of detecting plasma oscillations inside junctions is necessary to characterize the precise nature of the relation between fluxon flow patterns and the plasma excitation modes.

Acknowledgements

We appreciate helpful private communications with M. Tachiki. The underdoped single crystals were provided by N. Momono and M. Ido in Hokkaido University. This work was supported by National Research Laboratory Project administered by Korea Institute of Science and Technology Evaluation and Planning, the Center for Excellency (SRC) administered by Korea Science and Engineering Foundation, and Microwave

Application Research Center administered by The Agency for Defense Development. This study is also partly supported by KRISS.

References

[1] A.V. Ustinov, Physica D 123 (1998) 315, and references therein.
[2] N.F. Pedersen, A.V. Ustinov, Supercond. Sci. Technol. 8 (1995) 389, and references therein.
[3] R. Kleiner, Phys. Rev. B 50 (1994) 6919.
[4] R. Kleiner, P. Müller, H. Kohlstedt, N.F. Pedersen, S. Sakai, Phys. Rev. B 50 (1994) 3942.
[5] R. Kleiner, P. Müller, Phys. Rev. B 49 (1994) 1327.
[6] S. Sakai, P. Bodin, N.F. Pedersen, J. Appl. Phys. 73 (1993) 2411.
[7] S. Sakai, A.V. Ustinov, H. Kohlstedt, A. Petraglia, N.F. Pedersen, Phys. Rev. B 50 (1994) 12905;
S. Sakai, A.V. Ustinov, N. Thyssen, H. Kohlstedt, Phys. Rev. B 58 (1998) 5777.
[8] M. Machida, T. Koyama, M. Tachiki, Phys. Rev. Lett. 83 (1999) 4618.
[9] D.A. Ryndyk, Phys. Rev. Lett. 80 (1998) 3376.
[10] A.V. Ustinov, H. Kohlstedt, Phys. Rev. B 54 (1996) 6111.
[11] A.V. Ustinov, S. Sakai, Appl. Phys. Lett. 73 (1998) 686.
[12] M. Tachiki, M. Machida, Physica C 341–348 (2000) 1493.
[13] N.F. Pedersen, S. Sakai, Phys. Rev. B 58 (1998) 2820.
[14] V.P. Koshelets, S.V. Shitov, A.M. Baryshev, I.L. Lapitskaya, L.V. Filippenko, H. van de Stadt, J. Mees, H. Schaeffer, T. de Graauw, IEEE Trans. Appl. Supercond. 5 (1995) 3057;
W. Walkenhorst, G. Hechtfischer, S. Schlotzer, R. Kleiner, P. Müller, Phys. Rev. B 56 (1997) 8396.
[15] R. Kleiner, F. Steinmeyer, G. Kunkel, P. Müller, Phys. Rev. Lett. 68 (1992) 2394.
[16] J.U. Lee, P. Guptasarma, D. Hornbaker, A. El-Kortas, D. Hinks, K.E. Gray, Appl. Phys. Lett. 71 (1997) 1412.
[17] Y.-J. Doh, J. Kim, H.-S. Chang, S. Chang, H.-J. Lee, K.T. Kim, W. Lee, J.H. Choy, Phys. Rev. B 63 (2001) 144523.
[18] M. Machida, T. Koyama, A. Tanaka, M. Tachiki, Physica C 330 (2000) 85.
[19] M. Machida, T. Koyama, M. Tachiki, Physica C 362 (2001) 16.
[20] N. Kim, Y.-J. Doh, H.-S. Chang, H.-J. Lee, Physica C 341–348 (2002) 1563.
[21] A. Irie, Y. Hirai, G. Oya, Appl. Phys. Lett. 72 (1998) 2159;
H.B. Wang, Y. Aruga, T. Tachiki, Y. Mizugaki, J. Chen, K. Nakajima, T. Yamashita, P.H. Wu, Appl. Phys. Lett. 74 (1999) 3693;
V.M. Krasnov et al., Phys. Rev. B 59 (1999) 8463.
[22] G. Hechtfischer et al., Phys. Rev. Lett. 79 (1997) 1365.
[23] R. Kleiner, T. Gaber, G. Hechtfischer, Phys. Rev. B 62 (2000) 4086.
[24] V.M. Krasnov et al., Phys. Rev. B 59 (1999) 8463.
[25] H.-S. Chang, H.-J. Lee, M. Oda, Phys. Rev. B 64 (2001) 134504.
[26] G. Hechtfischer, R. Kleiner, K. Schlenga, W. Walkenhorst, P. Müller, Phys. Rev. B 55 (1997) 14638.
[27] Y.-J. Doh, J. Kim, K.-T. Kim, H.-J. Lee, Phys. Rev. B 61 (2000) R3834.
[28] M.R. Presland, J.L. Tallon, R.G. Buckley, R.S. Liu, N.E. Flower, Physica C 176 (1991) 95;
G.V.M. Williams, J.L. Tallon, R. Michalak, R. Dupree, Phys. Rev. B 54 (1996) R6909.
[29] H.B. Wang, P.H. Wu, T. Yamashita, Appl. Phys. Lett. 78 (2001) 4010.